

000                    **DELAYED            MOMENTUM            AGGREGATION:**  
 001                    **COMMUNICATION-EFFICIENT BYZANTINE-ROBUST**  
 002                    **FEDERATED LEARNING WITH PARTIAL PARTICIPA-**  
 003                    **TION**

008                    **Anonymous authors**

009                    Paper under double-blind review

012                    **ABSTRACT**

014                    Federated Learning (FL) allows distributed model training across multiple clients  
 015                    while preserving data privacy, but it remains vulnerable to Byzantine clients that  
 016                    exhibit malicious behavior. While existing Byzantine-robust FL methods provide  
 017                    strong convergence guarantees (e.g., to a stationary point in expectation) under  
 018                    Byzantine attacks, they typically assume full client participation, which is un-  
 019                    realistic due to communication constraints and client availability. Under partial  
 020                    participation, existing methods fail immediately after the sampled clients contain  
 021                    a Byzantine majority, creating a fundamental challenge for sparse communica-  
 022                    tion. First, we introduce *delayed momentum aggregation*, a novel principle where  
 023                    the server aggregates the most recently received gradients from non-participating  
 024                    clients alongside fresh momentum from active clients. Our optimizer D-Byz-  
 025                    SGDM (Delayed Byzantine-robust SGD with Momentum) implements this de-  
 026                    layed momentum aggregation principle for Byzantine-robust FL with partial par-  
 027                    ticipation. Remarkably, experiments on deep learning tasks showed our method  
 028                    not only maintained stable convergence under various Byzantine attacks, but also  
 029                    outperformed standard FL methods with partial participation in non-Byzantine  
 030                    settings.

032                    **1 INTRODUCTION**

034                    Federated Learning (FL) enables collaborative training across many clients without centralizing  
 035                    raw data, and has become a standard approach when privacy, bandwidth, or governance constraints  
 036                    prevent data pooling (Kairouz et al., 2021; McMahan et al., 2017). Its central idea is to transmit  
 037                    gradients rather than raw data. Specifically, each client computes the gradient using their local dataset  
 038                    and sends it to the central server. Then, the central server computes the average of the gradients  
 039                    and updates the parameters. Since its proposal, FL has attracted many optimization researchers and  
 040                    has been widely studied in areas such as communication compression (Mishchenko et al., 2024;  
 041                    Khirirat et al., 2018; Horváth et al., 2023; Stich et al., 2018; Alistarh et al., 2017; Albasyoni et al.,  
 042                    2020; Li et al., 2021; Fatkhullin et al., 2023), data heterogeneity (Karimireddy et al., 2020b; Pu &  
 043                    Nedić, 2021; Takezawa et al., 2022; Cheng et al., 2024; Li et al., 2020; Yang et al., 2021; Wang  
 044                    et al., 2020; Zhang et al., 2021; Haddadpour et al., 2021; Alghunaim, 2024), accelerated methods  
 045                    (Kovalev et al., 2022; Jiang et al., 2024; d'Aspremont et al., 2021; Güler, 1992; Nesterov, 2018; Lin  
 046                    et al., 2015; Monteiro & Svaiter, 2013), and Byzantine-robust FL, including defenses for homoge-  
 047                    neous data (Blanchard et al., 2017a; Mhamdi et al., 2018; Damaskinos et al., 2019; Yin et al., 2018;  
 048                    Pillutla et al., 2022; Bernstein et al., 2019; Alistarh et al., 2018; Mhamdi et al., 2021; Karimireddy  
 049                    et al., 2021) and heterogeneous data (Sattler et al., 2020; Xie et al., 2019b; Chen et al., 2018; Rajput  
 050                    et al., 2019; Data & Diggavi, 2021a;b; Li et al., 2019; Acharya et al., 2022; El-Mhamdi et al., 2021;  
 Yang & Li, 2021; Allouah et al., 2023).

051                    Due to the nature of FL, where a large number of clients participate in the training process, it is  
 052                    vulnerable to clients that behave incorrectly, commonly referred to as Byzantine clients (Kairouz  
 053                    et al., 2021; Lamport et al., 2019). For instance, some clients may be faulty, while others may act  
 maliciously to disrupt training. Under Byzantine failures, naive averaging is notoriously brittle:

even a single Byzantine client can significantly skew the aggregated model updates. To address this issue, a large body of work has proposed Byzantine-robust FL methods (Blanchard et al., 2017a;b; Allouah et al., 2023; Karimireddy et al., 2021), which replace simple averaging with robust aggregation rules at the central server. A robust aggregator guarantees that, as long as the majority of inputs come from honest clients, the aggregation output remains close to the true average of the honest clients' parameters, regardless of the values sent by malicious clients. Thanks to these robust aggregation techniques, Byzantine-robust FL can maintain convergence guarantees, despite the presence of Byzantine clients.

However, most of these existing Byzantine-robust FL methods rely on the assumption that all clients participate in every round, which is unrealistic. Some clients may be temporarily unavailable, for example, due to unreliable connections or competing computational tasks (Kairouz et al., 2021; Bonawitz et al., 2017; Niu et al., 2020; Yan et al., 2024; Gu et al., 2021; Wang & Ji, 2022). Even if all clients were available, it is common practice to sample only a subset of the clients to reduce the communication overhead between the central server and the clients (Karimireddy et al., 2020b;a; Patel et al., 2022). When only a subset of clients participates, most existing Byzantine-robust FL methods fail to remain robust against Byzantine clients. Specifically, in the partial participation setting, the majority of the sampled clients can be malicious. In such a case, a robust aggregator may no longer provide a good estimation of the average of the honest clients' parameters. Only a few papers have studied Byzantine-robust FL with partial participation (Allouah et al., 2024; Malinovsky et al., 2024). Malinovsky et al. (2024) proposed a MARINA-style (SVRG/SAGA-family) optimizer with a specialized clipping strategy, showing tolerance even in rounds with a Byzantine majority. However, such MARINA/SVRG/SAGA or periodic full-gradient / large-minibatch schemes perform poorly for deep learning models (Defazio & Bottou, 2019). Allouah et al. (2024) proposed replacing the naive averaging in FedAvg (McMahan et al., 2017) with a Byzantine-robust aggregator. Their algorithm, however, relies on vanilla (non-momentum) SGD, which is vulnerable to time-coupled attacks (Baruch et al., 2019; Karimireddy et al., 2021), and it offers no mitigation when Byzantine clients form a majority.

In this paper, we tackle the challenge of Byzantine-robust FL with partial participation, aiming for a simple and practical solution. Our proposed method, D-Byz-SGDM (Delayed Byzantine-robust SGD with Momentum), is strikingly simple: at each aggregation step, the central server aggregates not only the gradients sent from the sampled clients but also the most recently received gradients from the non-sampled clients. As a result, this effectively aggregates the entire set of clients, thereby ensuring that the aggregation in which Byzantine clients constitute a majority never occurs during the training. Experiments on deep learning tasks show stable and robust training under both partial participation and Byzantine attacks.

We provide a comprehensive discussion of related work in Section 2 and proceed with the formal problem setup.

## 2 RELATED WORK

**Byzantine-robust FL under full participation.** Classical defenses replace naive averaging by robust aggregation rules such as Krum (Blanchard et al., 2017a), coordinate-wise median and trimmed-mean (Blanchard et al., 2017b), and geometric–median–based RFA (Pillutla et al., 2022); meta-rules like Bulyan further reduce adversarial leverage (Mhamdi et al., 2018). Yet these per-round defenses can be vulnerable to time-coupled attacks that inject small, undetectable biases which accumulate across rounds (Baruch et al., 2019; Xie et al., 2019a). A key development is to leverage history: Karimireddy et al. (2021) formalize such time-coupled failures and prove that momentum (together with robust aggregation) provably restores convergence; subsequent works refine the momentum view and resilient averaging (Farhadkhani et al., 2022). Heterogeneity (non-IID client data) exacerbates the problem: bucketing (Karimireddy et al., 2022) and nearest-neighbor mixing (NNM) (Allouah et al., 2023) are pre-aggregation mechanisms that systematically adapt IID-optimal rules (e.g., Krum, median, RFA) to the heterogeneous regime, closing gaps between achievable rates and lower bounds. Beyond aggregation, algorithmic alternatives include coding-theoretic redundancy (DRACO) (Chen et al., 2018) and filtering for non-convex objectives (Allen-Zhu et al., 2021; Alistarh et al., 2018). Complementing these meta-aggregation approaches that assume full participation, Dahan & Levy (2024b) propose an efficient *Centered Trimmed Meta*-

108 *Aggregator* (CTMA) that upgrades base robust aggregators to order-optimal performance at near-  
 109 averaging cost, and couple it with a double-momentum estimator to establish theoretical guarantees  
 110 within the stochastic convex optimization (SCO) framework for synchronous (full-participation)  
 111 training.

112

113

114

**Partial participation, and local updates.** Partial participation makes robustness strictly harder  
 115 because the sampled set occasionally contains a Byzantine majority. Early theory coupling Byzantine  
 116 robustness with local steps shows that convergence can be ensured only when the sampled cohort  
 117 has a sufficiently large honest fraction at each synchronization, e.g.,  $\varepsilon \leq 1/3$  corrupted among the  
 118  $K$  active clients (Data & Diggavi, 2021b, Thm. 1), an assumption strained by client sampling. The  
 119 interaction between client sampling, multiple local steps, and robust aggregation has since been an-  
 120 alyzed in detail by Allouah et al. (2024), who quantifies how client sampling reshapes the effective  
 121 number of Byzantine clients and shows regimes where standard robust aggregators suffice; however,  
 122 these schemes omit momentum and do not mitigate time-coupled drift. Another concurrent line  
 123 uses explicit MARINA/SVRG/SAGA periodic full-gradient/reference-gradient steps: by coupling  
 124 robust aggregation with gradient-difference clipping and periodic full-gradient steps, Malinovsky  
 125 et al. (2024) proves tolerance even when a sampled round is entirely Byzantine, at the cost of peri-  
 126 odic heavier steps. From a statistical-efficiency angle, protocols with near-optimal rates under full  
 127 participation have been derived via modern robust statistics (Zhu et al., 2023), and recent work ex-  
 128 plores communication compression jointly with robustness (Rammal et al., 2024; Gorbunov et al.,  
 129 2023).

130

131

**Connection to MIFA.** MIFA (Gu et al., 2021) tackles arbitrary client unavailability by caching  
 132 each client’s latest update and substituting this surrogate when the client is absent, followed by  
 133 naive averaging. Within our framework this is the instantiation where the robust aggregator is re-  
 134 placed by the mean and the client-side momentum weight is fixed at  $\alpha = 1$ , i.e., cached updates are  
 135 used without attenuation. In our analysis this corresponds to a robustness constant  $c = \infty$ , making  
 136 our generic upper bound vacuous and reflecting that naive averaging cannot deliver Byzantine guar-  
 137 antees. Moreover, MIFA omits momentum; even if paired with a robust aggregator, the lower bound  
 138 of Karimireddy et al. (2021) would still apply, as momentum is necessary to overcome time-coupled  
 139 Byzantine drift.

140

141

142

**Asynchrony, delayed gradients, and relevance to our staleness mechanism.** Analysis of asyn-  
 143 chronous SGD (ASGD) formalizes *delayed/stale* gradients and shows that delays can be controlled  
 144 via delay-aware stepsizes (Koloskova et al., 2022; Mishchenko et al., 2022). In the *Byzantine*  
 145 *asynchronous* regime, recent work Dahan & Levy (2024a) develops a *weighted* robust-aggregation  
 146 framework and, combined with a double-momentum estimator, proves optimal convergence in the  
 147 smooth *convex homogeneous* (i.i.d.) setting (Dahan & Levy, 2024a). Importantly for assumptions,  
 148 Dahan & Levy (2024a;b)’s analysis (both asynchronous and synchronous) operates over a *compact*  
 149 feasible set (bounded diameter), which is stricter than the bounded-gradient conditions commonly  
 150 adopted in FL theory.

151

Our setting is not asynchronous; nevertheless, partial participation induces *server-side staleness*  
 152 because non-sampled clients contribute historical (per-client) gradients. This places our analysis  
 153 close to the ASGD toolbox while tackling a distinct failure mode (occasional Byzantine-majority  
 154 samples under subsampling) without trusted validation data. Technically, we leverage *per-client*  
 155 stale gradients to preserve a history-coupled (global) momentum across rounds, complementing  
 156 weighted robust aggregation in the asynchronous literature (Dahan & Levy, 2024a).

157

158

159

160

161

Relative to prior momentum-based defenses (Karimireddy et al., 2021; Farhadkhani et al., 2022)  
 and heterogeneity fixes (Karimireddy et al., 2022; Allouah et al., 2023), we study the regime  
 where clients refresh stochastically and Byzantine clients can transiently comprise the sampled  
 majority. Compared to MARINA/SVRG/SAGA-style periodic full-gradient/reference-gradient ap-  
 proaches (Malinovsky et al., 2024), our method avoids periodic full-batch gradient computations,  
 making it more practical and scalable for real federated learning deployments.

162 

### 3 PRELIMINARY

163

164 

**Notations.** Our notation largely follows (Koloskova et al., 2020; Karimireddy et al., 2022). We  
165 denote by  $n$  the total number of clients, and for any positive integer  $k$ , let  $[k] := \{1, 2, \dots, k\}$ .  
166 The set of good (non-Byzantine) clients is represented by  $\mathcal{G} \subseteq [n]$  with cardinality  $G := |\mathcal{G}|$ . The  
167 Byzantine ratio is defined as  $\delta := (n - G)/n$ , and throughout this paper we assume  $\delta < 1/2$ . For  
168 each client  $i$ , let  $\mathcal{D}_i$  denote the distribution of local data  $\xi_i$  over parameter space  $\Omega_i$ . The local loss  
169 function is given by  $f_i : \mathbb{R}^d \rightarrow \mathbb{R}$ , defined as  $f_i(x) := \mathbb{E}_{\xi_i}[F_i(x; \xi_i)]$  where  $F_i : \mathbb{R}^d \times \Omega_i \rightarrow \mathbb{R}$  is  
170 the sample loss.

171 

**Problem Definition.** We formalize the problem as follows:

172 
$$\min_{x \in \mathbb{R}^d} \left\{ f(x) := \frac{1}{G} \sum_{i \in \mathcal{G}} f_i(x) \right\}$$
173

174 where  $x \in \mathbb{R}^d$  denotes the model parameters and  $\mathcal{D}_i$  represents the dataset distribution of client  $i$ .  
175 In general,  $\mathcal{D}_i \neq \mathcal{D}_j$ , reflecting data heterogeneity across clients.

176 

**Byzantine-robust Learning under Full-Participation** The full participation setting serves as the  
177 theoretical foundation for Byzantine-robust federated learning, where the fundamental challenge is  
178 designing aggregation mechanisms that maintain convergence guarantees despite adversarial behav-  
179 ior. This setting provides clean theoretical analysis by eliminating client sampling complexities,  
180 establishing design principles for robust aggregation rules and performance benchmarks that inform  
181 practical algorithm design. The case of full client participation has been extensively studied in the  
182 literature (Karimireddy et al., 2022; Allouah et al., 2023; Gorbunov et al., 2023).

183 In this setting, robustness is typically achieved by replacing the simple average with a robust aggre-  
184 gation rule. While the precise definition of such aggregators may vary across works, we adopt the  
185 following notion from Karimireddy et al. (2022) and use it throughout this paper.

186 

**Assumption 1**  $((\delta, c)$ -Robust Aggregator (Karimireddy et al., 2022; Malinovsky et al., 2024)). Let  
187  $\{X_1, X_2, \dots, X_n\}$  be a set of random vectors. Suppose there exists a “good” subset  $\mathcal{G} \subseteq [n]$  of size  
188  $G = |\mathcal{G}| > n/2$  such that

189 
$$\mathbb{E}\|X_i - X_j\|^2 \leq \rho^2, \forall i, j \in \mathcal{G}.$$

190 Then the output  $\hat{X}$  of a Byzantine-robust aggregator  $\text{Agg}$  satisfies

191 
$$\mathbb{E}\|\text{Agg}(X_1, \dots, X_n) - \bar{X}\|^2 \leq c\delta\rho^2, \text{ where } \bar{X} = \frac{1}{G} \sum_{i \in \mathcal{G}} X_i.$$
192

193 Importantly, this definition is not merely abstract. Karimireddy et al. (2022) prove (in Theorem 1)  
194 that well-known aggregation rules such as KRUM (Blanchard et al., 2017a), RFA (Pillutla et al.,  
195 2022), and the coordinate-wise median, when combined with their proposed *bucketing* technique,  
196 indeed satisfy Assumption 1. Thus, concrete and practical instantiations of robust aggregators are  
197 available within this framework. In addition, momentum-based or explicit MARINA/SVRG/SAGA  
198 periodic full-gradient (or large-minibatch) techniques (Gorbunov et al., 2023; Rammal et al., 2024)  
199 are necessary to achieve robustness against sophisticated attacks. While heavy-ball momentum it-  
200 self can be interpreted as a form of variance reduction (Cutkosky & Orabona, 2019), throughout  
201 this paper we refer to heavy-ball-style updates simply as momentum. Without such techniques,  
202 Karimireddy et al. (2021) showed a fundamental lower bound demonstrating that learning fails when  
203 stochastic gradient noise is not properly controlled, making these methods essential for countering  
204 time-coupled attacks (Baruch et al., 2019).

205 

**Federated Learning with Partial Participation** Federated learning with partial participation is  
206 a fundamental characteristic of practical federated learning systems. Real-world deployments in-  
207 herently involve clients with heterogeneous capabilities and intermittent availability due to device  
208 constraints, battery limitations, and network connectivity variations (McMahan et al., 2017; Kairouz  
209 et al., 2021). This participation pattern directly impacts communication efficiency and system scal-  
210 ability, making it a critical consideration for algorithm design.

In the usual partial participation setting, all clients are assumed to be non-Byzantine, i.e.,  $\mathcal{G} = [n]$ . The classical FEDAVG algorithm (McMahan et al., 2017) samples a subset of active clients, denoted by  $\mathcal{S}_t \subseteq [n]$ , uniformly at random at each round  $t$ , and aggregates their local updates by naive averaging:  $\frac{1}{|\mathcal{S}_t|} \sum_{i \in \mathcal{S}_t} g_i^t$ , where  $g_i^t$  denotes the local gradient estimator of client  $i$  (e.g., a stochastic gradient).

**Failure of Byzantine-robust Learning with Partial Participation** A natural extension of the full participation setting is to replace the naive averaging step

$$\frac{1}{|\mathcal{S}_t|} \sum_{i \in \mathcal{S}_t} g_i^t \longrightarrow \text{Agg}(\{g_i^t\}_{i \in \mathcal{S}_t}).$$

While appealing, **this strategy fails with partial participation**: in some rounds, the sampled set may contain a Byzantine majority, despite the global condition  $\delta < 1/2$ . Under the (standard) model where the server only receives the gradients/momenta submitted in that round and has no additional side information, no (per-round) robust aggregator can reliably distinguish adversarial updates from honest updates when the sampled set contains a Byzantine majority. Furthermore, if we consider i.i.d. Bernoulli sampling, the likelihood of the existence of at least one round containing a Byzantine-majority grows exponentially with time.

Recent work has sought to address this issue. Allouah et al. (2024) provided lower bounds on the subsample size. However, due to a lack of momentum or large-minibatch sampling, their method collapses under time-coupled attacks such as ALIE (Baruch et al., 2019). Malinovsky et al. (2024) established convergence guarantees tolerating Byzantine-majority rounds via gradient-difference clipping, but their analysis relies on MARINA/SVRG/SAGA-style periodic full-gradient optimizers, which are known to be ineffective in deep learning (Defazio & Bottou, 2019).

## 4 PROPOSED METHOD

In this section, we propose **delayed momentum aggregation**, which is to apply the robust aggregator not only to the momentum of sampled clients but also to the cached momentum of non-sampled clients. Then, we propose a delayed momentum aggregation-based optimizer D-Byz-SGDM, which is Byzantine-robust even if only a subset of clients participate in each round. Formally, let  $x^t$  denote the global model parameter maintained by the server at round  $t$ . The server then updates it using delayed momentum aggregation as follows:

$$x^t = x^{t-1} - \eta \text{ Agg} \left( \{m_i^t\}_{i \in \mathcal{S}_t} \cup \{m_i^{t-\tau(i,t)}\}_{i \in [n] \setminus \mathcal{S}_t} \right), \quad (\text{delayed momentum aggregation})$$

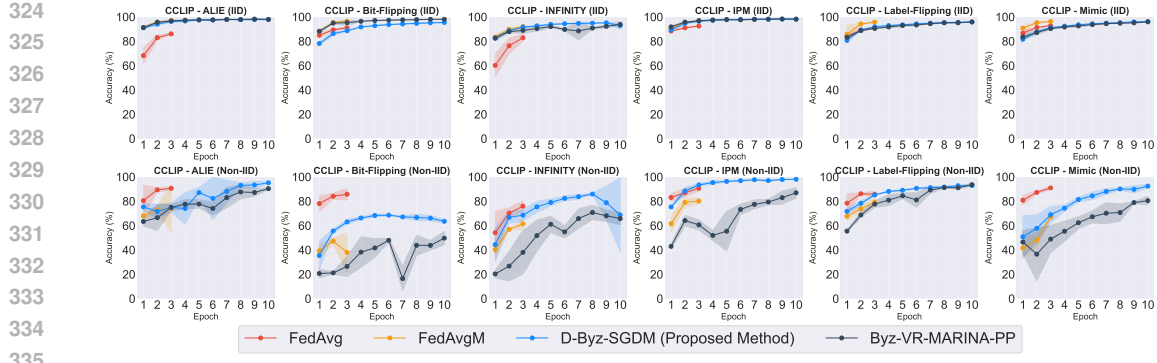
where each  $m_i^t$  represents a local momentum estimate, and  $\tau(i,t)$  denotes the (possibly stochastic) delay since client  $i$ 's last update was received. This design maintains that  $\text{Agg}(\cdot)$  consistently sees the global Byzantine fraction  $\delta < 1/2$ , ensuring robustness even with partial participation.

As a concrete special case of the main idea, we propose a new method, D-Byz-SGDM, whose update rule is given in Algorithm 1. In each round  $t$ , the server independently samples each client with probability  $p$  (i.e.,  $z^t \sim \text{Ber}(p)^{\otimes n}$  and  $\mathcal{S}_t = \{i : z_i^t = 1\}$ ). The selected clients refresh their momentum, while non-selected clients retain their cached value:

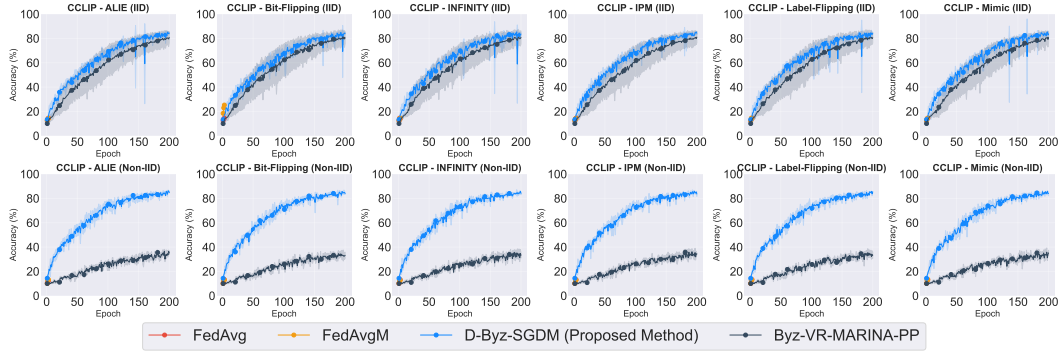
$$m_i^t = \begin{cases} (1 - \alpha)m_i^{t-1} + \alpha \nabla f_i(x^{t-1}, \xi_i^{t-1}), & i \in \mathcal{S}_t, \\ m_i^{t-1}, & i \notin \mathcal{S}_t, \end{cases}$$

where  $\alpha \in (0, 1]$  is the client momentum parameter. Note that each client  $i$  is included in  $\mathcal{S}_t$  with probability  $p$ . Importantly, D-Byz-SGDM introduces no extra communication overhead. The server simply maintains one vector  $m_i^t$  per client while reusing cached momentum for non-sampled clients, resulting in a memory requirement matching the full participation setting. As a possible mitigation for extreme cross-device regimes, one could explore streaming robust mean estimators (e.g., the streaming-based robust aggregator of Diakonikolas et al. (2022)) to shrink the server-side memory footprint, though such techniques are not yet compatible with our current robust aggregation definition, and we leave this integration for future work.





(a) MNIST under centered clipping (CCLIP). The top row shows IID splits and the bottom row shows non-IID splits with bucketing  $s = 2$ ; from left to right the columns correspond to ALIE, Bit-Flipping, INFINITY, IPM, Label-Flipping, and Mimic attacks. *Observation:* D-Byz-SGDM remains the most stable and accurate across all attacks, while FedAvg/FedAvgM diverge when many Byzantines are sampled.



(b) CIFAR-10 (ResNet-18) under centered clipping (CCLIP). The top row reports IID splits and the bottom row reports non-IID splits with bucketing  $s = 2$ ; moving left to right the columns correspond to ALIE, Bit-Flipping, INFINITY, IPM, Label-Flipping, and Mimic attacks. *Observation:* D-Byz-SGDM sustains 80–85% accuracy across attacks, whereas FedAvg/FedAvgM often collapse by epoch  $\approx 4$  when a Byzantine majority is sampled.

Figure 1: Byzantine-robust training with CCLIP and partial participation ( $p = 0.5$ ). D-Byz-SGDM is consistently the most accurate and stable curve.

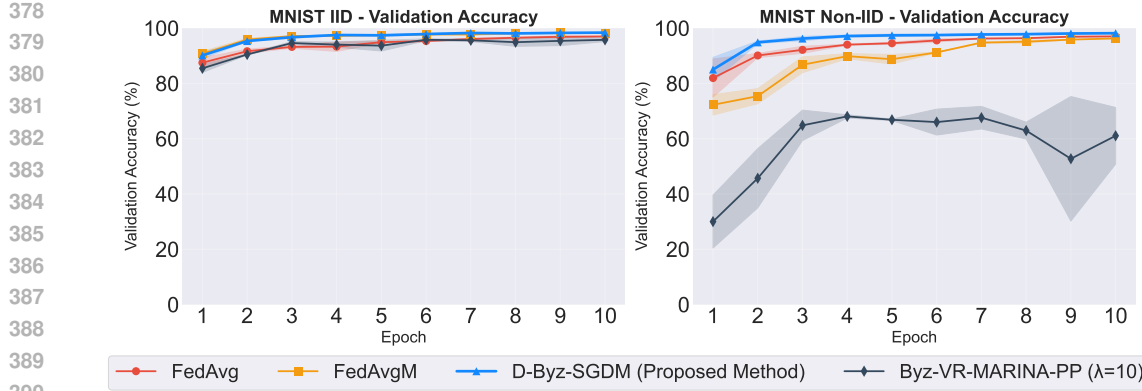
MNIST (lower half of Fig. 1a), Byz-VR-MARINA-PP exhibited high variance and unstable convergence, while D-Byz-SGDM maintained consistent performance. The disparity was dramatic on non-IID CIFAR-10 (lower half of Fig. 1b): Byz-VR-MARINA-PP catastrophically failed (20–35% accuracy), whereas D-Byz-SGDM maintained 80–85% accuracy. The delayed momentum aggregation principle proved crucial. While standard methods failed when a Byzantine majority was sampled,<sup>2</sup> D-Byz-SGDM maintained stable convergence. (3) *The approach generalizes across aggregators.* Similar trends held across other aggregators (avg, krum, cm, rfa) and both datasets, with FedAvg and FedAvgM performing poorly in both IID and non-IID settings (FedAvgM showed marginal improvements only in specific attacks like Bit-Flipping); see Appendix D for the full set of figures.

## 5.2 BASELINE PERFORMANCE WITHOUT BYZANTINE CLIENTS

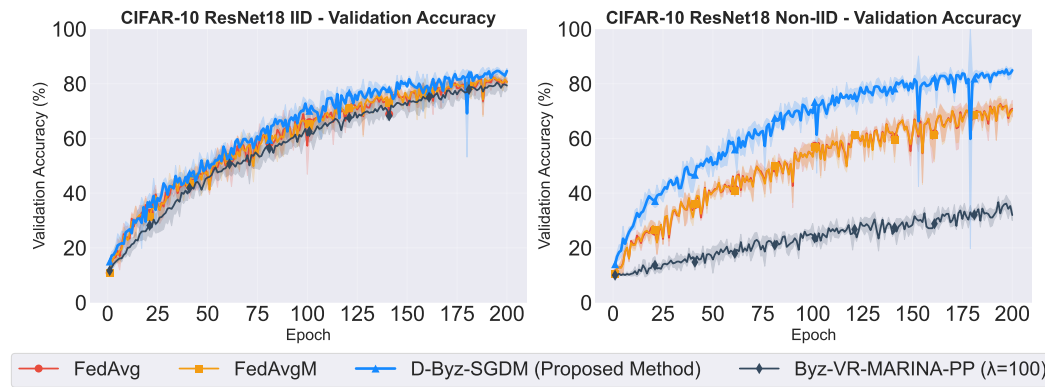
We also examined the non-Byzantine setting ( $\delta = 0$ ) to establish baseline performance. The setup used  $n = 20$  clients with the avg aggregator. The results were summarized in Figures 2a and 2b.

**Key findings.** Across both IID and non-IID settings on MNIST (Fig. 2a), Byz-VR-MARINA-PP achieved the worst validation accuracy and highest loss throughout training. Surprisingly, D-Byz-SGDM consistently outperformed FedAvgM in the non-Byzantine setting ( $\delta = 0$ ), despite the risk that reusing momentum across rounds could degrade performance. The advantage persisted on the

<sup>2</sup>With  $p = 0.5$ , if many Byzantines were sampled together, they could overwhelm the aggregation.



(a) MNIST without Byzantine clients ( $\delta = 0$ ) using the `avg` aggregator. The left panel reports the IID partition and the right panel reports the non-IID partition. *Observation:* performance is saturated in IID; D-Byz-SGDM retains a clear margin in non-IID, showing delayed momentum aggregation mitigates heterogeneity even without attacks.



(b) CIFAR-10 / ResNet-18 without Byzantine clients ( $\delta = 0$ ) using the `avg` aggregator. The left panel shows the IID partition and the right panel shows the non-IID partition. *Observation:* D-Byz-SGDM converges faster and finishes 5–10 points higher on both partitions, while Byz-VR-MARINA-PP remains well below momentum baselines.

Figure 2: Baseline training with partial participation ( $p = 0.5$ ) and no Byzantine clients ( $\delta = 0$ ). Delayed momentum aggregation (D-Byz-SGDM) remains strongest in non-IID even without adversaries.

deeper model (ResNet-18) on CIFAR-10 (Fig. 2b), underscoring that delayed momentum aggregation scaled beyond vision tasks with shallow networks. The curves suggested that with partial participation ( $p = 0.5$ ) and heterogeneity (non-IID), the delayed momentum aggregation mechanism in D-Byz-SGDM mitigated heterogeneity-induced drift, acting as an *implicit regularizer* even without attacks. We further examined Byz-VR-MARINA-PP in the non-Byzantine regime. Somewhat unexpectedly, applying clipping to momentum differences introduced a *bias* detrimental to performance unless the clipping hyperparameter  $\lambda$  was chosen with extreme care. This sensitivity highlighted a trade-off: while clipping was essential to defend against Byzantine behaviors, it could significantly distort gradient estimates in non-Byzantine settings.

## 6 CONCLUSION

We proposed *delayed momentum aggregation*, a novel principle where servers aggregate fresh momentum from participating clients with the most recently received momentum from non-participating clients. Our D-Byz-SGDM optimizer maintains Byzantine-robustness under partial participation while remaining lightweight to deploy. Experiments showed consistent improvements over existing methods across various attacks and data distributions. The delayed momentum aggregation principle opens promising avenues for extension to other client selection schemes (Fraboni

432 et al., 2022; Cho et al., 2020; Fraboni et al., 2021; Li et al., 2020; Chen et al., 2022) beyond Bernoulli  
 433 sampling.  
 434

435 **ETHICS STATEMENT**  
 436

438 This work addresses robustness in federated learning against adversarial participants. We use  
 439 “Byzantine” following established distributed systems nomenclature to denote arbitrary failures,  
 440 with no cultural reference intended. Our proposed method is defensive, designed to enhance the  
 441 reliability and safety of collaborative training.  
 442

443 **REFERENCES**  
 444

445 Anish Acharya, Abolfazl Hashemi, Prateek Jain, Sujay Sanghavi, Inderjit S. Dhillon, and Ufuk  
 446 Topcu. Robust training in high dimensions via block coordinate geometric median descent. In  
 447 *International Conference on Artificial Intelligence and Statistics*, 2022.

448 Alyazeed Albasyoni, Mher Safaryan, Laurent Condat, and Peter Richtárik. Optimal gradient com-  
 449 pression for distributed and federated learning. *ArXiv preprint*, abs/2010.03246, 2020.

450 Sulaiman A. Alghunaim. Local exact-diffusion for decentralized optimization and learning. *IEEE*  
 451 *Transactions on Automatic Control*, 69(11):7371–7386, 2024.

452 Dan Alistarh, Demjan Grubic, Jerry Li, Ryota Tomioka, and Milan Vojnovic. QSGD:  
 453 communication-efficient SGD via gradient quantization and encoding. In *Advances in Neural*  
 454 *Information Processing Systems*, 2017.

455 Dan Alistarh, Zeyuan Allen-Zhu, and Jerry Li. Byzantine stochastic gradient descent. In *Advances*  
 456 *in Neural Information Processing Systems*, 2018.

457 Zeyuan Allen-Zhu, Faeze Ebrahimianghazani, Jerry Li, and Dan Alistarh. Byzantine-resilient non-  
 458 convex stochastic gradient descent. In *International Conference on Learning Representations*,  
 459 2021.

460 Youssef Allouah, Sadegh Farhadkhani, Rachid Guerraoui, Nirupam Gupta, Rafael Pinot, and John  
 461 Stephan. Fixing by mixing: A recipe for optimal byzantine ML under heterogeneity. In *Interna-*  
 462 *tional Conference on Artificial Intelligence and Statistics*, 2023.

463 Youssef Allouah, Sadegh Farhadkhani, Rachid Guerraoui, Nirupam Gupta, Rafael Pinot, Geovani  
 464 Rizk, and Sasha Voitovych. Byzantine-robust federated learning: Impact of client subsampling  
 465 and local updates. In *International Conference on Machine Learning*, 2024.

466 Gilad Baruch, Moran Baruch, and Yoav Goldberg. A little is enough: Circumventing defenses for  
 467 distributed learning. In *Advances in Neural Information Processing Systems*, 2019.

468 Jeremy Bernstein, Jiawei Zhao, Kamyar Azizzadenesheli, and Anima Anandkumar. signsgd with  
 469 majority vote is communication efficient and fault tolerant. In *International Conference on Learn-*  
 470 *ing Representations*, 2019.

471 Peva Blanchard, El Mahdi El Mhamdi, Rachid Guerraoui, and Julien Stainer. Machine learning with  
 472 adversaries: Byzantine tolerant gradient descent. In *Advances in Neural Information Processing*  
 473 *Systems*, 2017a.

474 Peva Blanchard, El Mahdi El Mhamdi, Rachid Guerraoui, and Julien Stainer. Machine learning with  
 475 adversaries: Byzantine tolerant gradient descent. In *Advances in Neural Information Processing*  
 476 *Systems*, 2017b.

477 Kallista A. Bonawitz, Vladimir Ivanov, Ben Kreuter, Antonio Marcedone, H. Brendan McMahan,  
 478 Sarvar Patel, Daniel Ramage, Aaron Segal, and Karn Seth. Practical secure aggregation for  
 479 privacy-preserving machine learning. In *ACM SIGSAC Conference on Computer and Commu-*  
 480 *nications Security*, pp. 1175–1191, 2017.

486 Lingjiao Chen, Hongyi Wang, Zachary B. Charles, and Dimitris S. Papailiopoulos. DRACO:  
 487 byzantine-resilient distributed training via redundant gradients. In *International Conference on*  
 488 *Machine Learning*, 2018.

489

490 Wenlin Chen, Samuel Horváth, and Peter Richtárik. Optimal client sampling for federated learning.  
 491 *Trans. Mach. Learn. Res.*, 2022.

492

493 Ziheng Cheng, Xinmeng Huang, Pengfei Wu, and Kun Yuan. Momentum benefits non-iid federated  
 494 learning simply and provably. In *International Conference on Learning Representations*, 2024.

495

496 Yae Jee Cho, Jianyu Wang, and Gauri Joshi. Client selection in federated learning: Convergence  
 497 analysis and power-of-choice selection strategies. *ArXiv preprint*, abs/2010.01243, 2020.

498

499 Ashok Cutkosky and Francesco Orabona. Momentum-based variance reduction in non-convex sgd.  
 500 *Advances in neural information processing systems*, 2019.

501

502 Tehila Dahan and Kfir Y. Levy. Weight for robustness: A comprehensive approach towards optimal  
 503 fault-tolerant asynchronous ML. In *Advances in Neural Information Processing Systems*, 2024a.

504

505 Tehila Dahan and Kfir Yehuda Levy. Fault tolerant ML: efficient meta-aggregation and synchronous  
 506 training. In *International Conference on Machine Learning*, 2024b.

507

508 Georgios Damaskinos, El-Mahdi El-Mhamdi, Rachid Guerraoui, Arsany Guirguis, and Sébastien  
 509 Rouault. AGGREGATHOR: byzantine machine learning via robust gradient aggregation. In  
 510 *Proceedings of Machine Learning and Systems*, 2019.

511

512 Alexandre d'Aspremont, Damien Scieur, and Adrien B. Taylor. Acceleration methods. *Found.  
 513 Trends Optim.*, 5(1-2):1–245, 2021.

514

515 Deepesh Data and Suhas N. Diggavi. Byzantine-resilient SGD in high dimensions on heterogeneous  
 516 data. In *IEEE International Symposium on Information Theory*, 2021a.

517

518 Deepesh Data and Suhas N. Diggavi. Byzantine-resilient high-dimensional SGD with local iterations  
 519 on heterogeneous data. In *International Conference on Machine Learning*, 2021b.

520

521 Aaron Defazio and Léon Bottou. On the ineffectiveness of variance reduced optimization for deep  
 522 learning. In *Advances in Neural Information Processing Systems*, 2019.

523

524 Ilias Diakonikolas, Daniel M Kane, Ankit Pensia, and Thanasis Pittas. Streaming algorithms for  
 525 high-dimensional robust statistics. In *International Conference on Machine Learning*, 2022.

526

527 El-Mahdi El-Mhamdi, Sadegh Farhadkhani, Rachid Guerraoui, Arsany Guirguis, Lê-Nguyễn  
 528 Hoang, and Sébastien Rouault. Collaborative learning in the jungle (decentralized, byzantine,  
 529 heterogeneous, asynchronous and nonconvex learning). In *Advances in Neural Information Pro-  
 530 cessing Systems*, 2021.

531

532 Sadegh Farhadkhani, Rachid Guerraoui, Nirupam Gupta, Rafael Pinot, and John Stephan. Byzantine  
 533 machine learning made easy by resilient averaging of momentums. In *International Conference  
 534 on Machine Learning*, 2022.

535

536 Ilyas Fatkhullin, Alexander Tyurin, and Peter Richtárik. Momentum provably improves error feed-  
 537 back! In *Advances in Neural Information Processing Systems*, 2023.

538

539 Yann Fraboni, Richard Vidal, Laetitia Kameni, and Marco Lorenzi. Clustered sampling: Low-  
 540 variance and improved representativity for clients selection in federated learning. In *International  
 541 Conference on Machine Learning*, 2021.

542

543 Yann Fraboni, Richard Vidal, Laetitia Kameni, and Marco Lorenzi. A general theory for client  
 544 sampling in federated learning. In *International Workshop on Trustworthy Federated Learning*.  
 545 Springer, 2022.

546

547 Marc González, Rachid Guerraoui, Rafael Pinot, Geovani Rizk, John Stephan, and François Taïani.  
 548 *Byzfl: Research framework for robust federated learning*, 2025.

540 Eduard Gorbunov, Samuel Horváth, Peter Richtárik, and Gauthier Gidel. Variance reduction is an  
 541 antidote to byzantines: Better rates, weaker assumptions and communication compression as a  
 542 cherry on the top. In *International Conference on Learning Representations*, 2023.

543

544 Xinran Gu, Kaixuan Huang, Jingzhao Zhang, and Longbo Huang. Fast federated learning in the  
 545 presence of arbitrary device unavailability. In *Advances in Neural Information Processing Sys-  
 546 tems*, 2021.

547 Osman Güler. New proximal point algorithms for convex minimization. *SIAM J. Optim.*, 2(4):  
 548 649–664, 1992.

549

550 Farzin Haddadpour, Mohammad Mahdi Kamani, Aryan Mokhtari, and Mehrdad Mahdavi. Feder-  
 551 ated learning with compression: Unified analysis and sharp guarantees. In *International Confer-  
 552 ence on Artificial Intelligence and Statistics*, 2021.

553

554 Samuel Horváth, Dmitry Kovalev, Konstantin Mishchenko, Peter Richtárik, and Sebastian U. Stich.  
 555 Stochastic distributed learning with gradient quantization and double-variance reduction. *Optim.  
 556 Methods Softw.*, 38(1):91–106, 2023.

557

558 Xiaowen Jiang, Anton Rodomanov, and Sebastian U. Stich. Stabilized proximal-point methods for  
 559 federated optimization. In *Advances in Neural Information Processing Systems*, 2024.

560

561 Peter Kairouz, H. Brendan McMahan, Brendan Avent, Aurélien Bellet, Mehdi Bennis, Arjun Nitin  
 562 Bhagoji, Kallista A. Bonawitz, Zachary Charles, Graham Cormode, Rachel Cummings, Rafael  
 563 G. L. D’Oliveira, Hubert Eichner, Salim El Rouayheb, David Evans, Josh Gardner, Zachary Gar-  
 564 rett, Adrià Gascón, Badih Ghazi, Phillip B. Gibbons, Marco Gruteser, Zaïd Harchaoui, Chaoyang  
 565 He, Lie He, Zhouyuan Huo, Ben Hutchinson, Justin Hsu, Martin Jaggi, Tara Javidi, Gauri Joshi,  
 566 Mikhail Khodak, Jakub Konečný, Aleksandra Korolova, Farinaz Koushanfar, Sanmi Koyejo,  
 567 Tancrède Lepoint, Yang Liu, Prateek Mittal, Mehryar Mohri, Richard Nock, Ayfer Özgür, Rasmus  
 568 Pagh, Hang Qi, Daniel Ramage, Ramesh Raskar, Mariana Raykova, Dawn Song, Weikang Song,  
 569 Sebastian U. Stich, Ziteng Sun, Ananda Theertha Suresh, Florian Tramèr, Praneeth Vepakomma,  
 570 Jianyu Wang, Li Xiong, Zheng Xu, Qiang Yang, Felix X. Yu, Han Yu, and Sen Zhao. Advances  
 571 and open problems in federated learning. *Found. Trends Mach. Learn.*, 14(1-2):1–210, 2021.

572

573 Sai Praneeth Karimireddy, Martin Jaggi, Satyen Kale, Mehryar Mohri, Sashank J Reddi, Sebas-  
 574 tian U Stich, and Ananda Theertha Suresh. Mime: Mimicking centralized stochastic algorithms  
 575 in federated learning. *ArXiv preprint*, abs/2008.03606, 2020a.

576

577 Sai Praneeth Karimireddy, Satyen Kale, Mehryar Mohri, Sashank J. Reddi, Sebastian U. Stich, and  
 578 Ananda Theertha Suresh. SCAFFOLD: stochastic controlled averaging for federated learning. In  
 579 *International Conference on Machine Learning*, 2020b.

580

581 Sai Praneeth Karimireddy, Lie He, and Martin Jaggi. Learning from history for byzantine robust  
 582 optimization. In *International Conference on Machine Learning*, 2021.

583

584 Sai Praneeth Karimireddy, Lie He, and Martin Jaggi. Byzantine-robust learning on heterogeneous  
 585 datasets via bucketing. In *International Conference on Learning Representations*, 2022.

586

587 Sarit Khirirat, Hamid Reza Feyzmahdavian, and Mikael Johansson. Distributed learning with com-  
 588 pressed gradients. *ArXiv preprint*, abs/1806.06573, 2018.

589

590 Anastasia Koloskova, Nicolas Loizou, Sadra Boreiri, Martin Jaggi, and Sebastian U. Stich. A uni-  
 591 fied theory of decentralized SGD with changing topology and local updates. In *International  
 592 Conference on Machine Learning*, 2020.

593

Anastasia Koloskova, Sebastian U. Stich, and Martin Jaggi. Sharper convergence guarantees for  
 594 asynchronous SGD for distributed and federated learning. In *Advances in Neural Information  
 595 Processing Systems*, 2022.

Dmitry Kovalev, Aleksandr Beznosikov, Ekaterina Borodich, Alexander V. Gasnikov, and Gesualdo  
 596 Scutari. Optimal gradient sliding and its application to optimal distributed optimization under  
 597 similarity. In *Advances in Neural Information Processing Systems*, 2022.

594 Leslie Lamport, Robert E. Shostak, and Marshall C. Pease. The byzantine generals problem. In  
 595 *Concurrency: the Works of Leslie Lamport*, pp. 203–226. 2019.  
 596

597 Liping Li, Wei Xu, Tianyi Chen, Georgios B. Giannakis, and Qing Ling. RSA: byzantine-robust  
 598 stochastic aggregation methods for distributed learning from heterogeneous datasets. In *AAAI*  
 599 *Conference on Artificial Intelligence*, 2019.

600 Tian Li, Anit Kumar Sahu, Manzil Zaheer, Maziar Sanjabi, Ameet Talwalkar, and Virginia Smith.  
 601 Federated optimization in heterogeneous networks. In *Proceedings of Machine Learning and*  
 602 *Systems*, 2020.

603

604 Zhize Li, Hongyan Bao, Xiangliang Zhang, and Peter Richtárik. PAGE: A simple and optimal prob-  
 605 abilistic gradient estimator for nonconvex optimization. In *International Conference on Machine*  
 606 *Learning*, 2021.

607 Hongzhou Lin, Julien Mairal, and Zaïd Harchaoui. A universal catalyst for first-order optimization.  
 608 In *Advances in Neural Information Processing Systems*, 2015.

609

610 Grigory Malinovsky, Peter Richtárik, Samuel Horváth, and Eduard Gorbunov. Byzantine robustness  
 611 and partial participation can be achieved at once: Just clip gradient differences. In *Advances in*  
 612 *Neural Information Processing Systems*, 2024.

613 Brendan McMahan, Eider Moore, Daniel Ramage, Seth Hampson, and Blaise Agüera y Arcas.  
 614 Communication-efficient learning of deep networks from decentralized data. In *International*  
 615 *Conference on Artificial Intelligence and Statistics*, 2017.

616

617 El Mahdi El Mhamdi, Rachid Guerraoui, and Sébastien Rouault. The hidden vulnerability of dis-  
 618 tributed learning in byzantium. In *International Conference on Machine Learning*, 2018.

619

620 El Mahdi El Mhamdi, Rachid Guerraoui, and Sébastien Rouault. Distributed momentum for  
 621 byzantine-resilient stochastic gradient descent. In *International Conference on Learning Rep-*  
 622 *resentations*, 2021.

623

624 Konstantin Mishchenko, Francis R. Bach, Mathieu Even, and Blake E. Woodworth. Asynchronous  
 625 SGD beats minibatch SGD under arbitrary delays. In *Advances in Neural Information Processing*  
 626 *Systems*, 2022.

627

628 Konstantin Mishchenko, Eduard Gorbunov, Martin Takáč, and Peter Richtárik. Distributed learning  
 629 with compressed gradient differences. *Optimization Methods and Software*, pp. 1–16, 2024.

630

631 Renato D. C. Monteiro and Benar Fux Svaiter. An accelerated hybrid proximal extragradient method  
 632 for convex optimization and its implications to second-order methods. *SIAM J. Optim.*, 23(2):  
 633 1092–1125, 2013.

634

635 Yurii Nesterov. *Lectures on convex optimization*. Springer, 2018.

636

637 Chaoyue Niu, Fan Wu, Shaojie Tang, Lifeng Hua, Rongfei Jia, Chengfei Lv, Zhihua Wu, and Guihai  
 638 Chen. Billion-scale federated learning on mobile clients: a submodel design with tunable privacy.  
 639 In *Annual International Conference on Mobile Computing and Networking*, 2020.

640

641 Kumar Kshitij Patel, Lingxiao Wang, Blake E. Woodworth, Brian Bullins, and Nati Srebro. To-  
 642 wards optimal communication complexity in distributed non-convex optimization. In *Advances*  
 643 *in Neural Information Processing Systems*, 2022.

644

645 Krishna Pillutla, Sham M. Kakade, and Zaïd Harchaoui. Robust aggregation for federated learning.  
 646 *IEEE Trans. Signal Process.*, 70:1142–1154, 2022.

647

648 Shi Pu and Angelia Nedić. Distributed stochastic gradient tracking methods. *Mathematical Pro-*  
 649 *gramming*, 187(1):409–457, 2021.

650

651 Shashank Rajput, Hongyi Wang, Zachary B. Charles, and Dimitris S. Papailiopoulos. DETOX: A  
 652 redundancy-based framework for faster and more robust gradient aggregation. In *Advances in*  
 653 *Neural Information Processing Systems*, 2019.

648 Ahmad Rammal, Kaja Gruntkowska, Nikita Fedin, Eduard Gorbunov, and Peter Richtárik. Commu-  
 649 nication compression for byzantine robust learning: New efficient algorithms and improved rates.  
 650 In *International Conference on Artificial Intelligence and Statistics*, 2024.

651

652 Felix Sattler, Klaus-Robert Müller, Thomas Wiegand, and Wojciech Samek. On the byzantine ro-  
 653 bustness of clustered federated learning. In *IEEE International Conference on Acoustics, Speech*  
 654 and *Signal Processing*, 2020.

655 Sebastian U. Stich, Jean-Baptiste Cordonnier, and Martin Jaggi. Sparsified SGD with memory. In  
 656 *Advances in Neural Information Processing Systems*, 2018.

657

658 Yuki Takezawa, Han Bao, Kenta Niwa, Ryoma Sato, and Makoto Yamada. Momentum tracking:  
 659 Momentum acceleration for decentralized deep learning on heterogeneous data. *Transactions on*  
 660 *Machine Learning*, 2022.

661 Jianyu Wang, Qinghua Liu, Hao Liang, Gauri Joshi, and H. Vincent Poor. Tackling the objective in-  
 662 consistency problem in heterogeneous federated optimization. In *Advances in Neural Information*  
 663 *Processing Systems*, 2020.

664 Shiqiang Wang and Mingyue Ji. A unified analysis of federated learning with arbitrary client par-  
 665 ticipation. In *Advances in Neural Information Processing Systems*, 2022.

666

667 Cong Xie, Oluwasanmi Koyejo, and Indranil Gupta. Fall of empires: Breaking byzantine-tolerant  
 668 SGD by inner product manipulation. In *Uncertainty in Artificial Intelligence*, 2019a.

669

670 Cong Xie, Sanmi Koyejo, and Indranil Gupta. Zeno: Distributed stochastic gradient descent with  
 671 suspicion-based fault-tolerance. In *International Conference on Machine Learning*, 2019b.

672

673 Yikai Yan, Chaoyue Niu, Yucheng Ding, Zhenzhe Zheng, Shaojie Tang, Qinya Li, Fan Wu, Chengfei  
 674 Lyu, Yanghe Feng, and Guihai Chen. Federated optimization under intermittent client availability.  
*INFORMS Journal on Computing*, 36(1):185–202, 2024.

675

676 Haibo Yang, Minghong Fang, and Jia Liu. Achieving linear speedup with partial worker partici-  
 677 pation in non-iid federated learning. In *International Conference on Learning Representations*,  
 678 2021.

679

680 Yi-Rui Yang and Wu-Jun Li. BASGD: buffered asynchronous SGD for byzantine learning. In  
*International Conference on Machine Learning*, 2021.

681

682 Dong Yin, Yudong Chen, Kannan Ramchandran, and Peter L. Bartlett. Byzantine-robust distributed  
 683 learning: Towards optimal statistical rates. In *International Conference on Machine Learning*,  
 2018.

684

685 Xinwei Zhang, Mingyi Hong, Sairaj V. Dhople, Wotao Yin, and Yang Liu. Fedpd: A federated  
 686 learning framework with adaptivity to non-iid data. *IEEE Transactions on Signal Processing*, 69:  
 687 6055–6070, 2021.

688

689 Banghua Zhu, Lun Wang, Qi Pang, Shuai Wang, Jiantao Jiao, Dawn Song, and Michael I. Jordan.  
 690 Byzantine-robust federated learning with optimal statistical rates. In *International Conference on*  
*Artificial Intelligence and Statistics*, 2023.

691

692

693

694

695

696

697

698

699

700

701

## 702 A LARGE LANGUAGE MODEL (LLM) USAGE

704 In accordance with ICLR 2026 guidelines, we disclose the use of Large Language Models (LLMs)  
 705 in preparing this submission:

- 707 • **Writing assistance:** Yes, LLMs were used to aid and polish writing. Specifically, we  
 708 employed LLMs to improve clarity, correct grammar, and enhance the overall presentation  
 709 of technical content throughout the manuscript. The authors take full responsibility for all  
 710 content, including any LLM-assisted portions.
- 711 • **Literature retrieval and discovery:** Yes, LLMs were used for finding related work. We  
 712 utilized LLMs to help identify relevant papers, understand connections between different  
 713 research areas, and ensure comprehensive coverage of the Byzantine-robust federated  
 714 learning literature. All citations were independently verified for accuracy.

715 We emphasize that all research ideas, algorithm design, experimental design, and results analysis  
 716 were conducted by the authors without LLM involvement. The LLMs served solely as auxiliary  
 717 tools for improving presentation and literature discovery.

## 719 B ALGORITHM DETAILS

722 We present the detailed algorithm for D-Byz-SGDM (Delayed Byzantine-robust SGD with Mo-  
 723 mentum), which implements our delayed momentum aggregation principle. The key idea is to apply the  
 724 robust aggregator not only to the momentum of sampled clients but also to the cached momentum  
 725 of non-sampled clients, ensuring that the aggregator consistently sees the global Byzantine fraction  
 726  $\delta < 1/2$  even under partial participation.

727 In each round  $t$ , the server independently samples each client with probability  $p$  (i.e.,  $z^t \sim \text{Ber}(p)^{\otimes n}$   
 728 and  $\mathcal{S}_t = \{i : z_i^t = 1\}$ ). The selected clients refresh their momentum using:

$$729 \quad m_i^t = \begin{cases} (1 - \alpha)m_i^{t-1} + \alpha \nabla f_i(x^{t-1}, \xi_i^{t-1}), & i \in \mathcal{S}_t, \\ 730 \quad m_i^{t-1}, & i \notin \mathcal{S}_t, \end{cases}$$

732 where  $\alpha \in (0, 1]$  is the client momentum parameter. Non-selected clients retain their cached mo-  
 733 mentum values from previous rounds.

735 The server then performs delayed momentum aggregation by applying the robust aggregator  $\text{Agg}$   
 736 to the union of fresh momentum from sampled clients and cached momentum from non-sampled  
 737 clients:

$$738 \quad m^t = \text{Agg}\left(\{m_i^t\}_{i \in \mathcal{S}_t} \cup \{m_i^t\}_{i \notin \mathcal{S}_t}\right)$$

739 This design ensures that even when partial participation might lead to a Byzantine majority among  
 740 sampled clients, the aggregator always operates on the full set of clients (fresh and cached), main-  
 741 taining robustness.

743 To see how this corresponds to the delayed momentum aggregation principle, note that the delay  
 744 function  $\tau(i, t)$  represents the number of rounds since client  $i$ 's momentum was last updated. For-  
 745 mally:

$$746 \quad \tau(i, t) = \min\{s \geq 0 : i \in \mathcal{S}_{t-s}\}$$

747 This is a random variable that depends on the sampling history. When  $i \in \mathcal{S}_t$ , we have  $\tau(i, t) = 0$   
 748 (fresh update), and when  $i \notin \mathcal{S}_t$ , we have  $\tau(i, t) > 0$  (stale update). The algorithm effectively  
 749 implements:

$$750 \quad x^t = x^{t-1} - \eta \text{Agg}\left(\{m_i^t\}_{i \in \mathcal{S}_t} \cup \{m_i^{t-\tau(i, t)}\}_{i \in [n] \setminus \mathcal{S}_t}\right)$$

751 where for non-sampled clients,  $m_i^{t-\tau(i, t)}$  is their most recent momentum update, which is exactly  
 752 what we store as  $m_i^t$  in the algorithm.

754 Importantly, D-Byz-SGDM does not incur additional communication costs compared to standard  
 755 partial participation methods: the server only queries sampled clients and stores one momentum  
 756 vector  $m_i^t$  per client, matching the memory requirements of full participation settings.

756 **C ADDITIONAL EXPERIMENTAL DETAILS**  
757758 **C.1 COMMON EXPERIMENTAL SETTINGS**  
759

760 All experiments covered two vision workloads: MNIST with a convolutional neural network archi-  
761 tecture (CONV-CONV-DROPOUT-FC-DROPOUT-FC) and CIFAR-10 with a standard ResNet-18.  
762 Training employed cross-entropy (negative log-likelihood) loss with batch size 32 per client and  
763 client participation probability  $p = 0.5$ . We evaluated both IID and non-IID data partitions, with  
764 the latter following the class-based approach of Karimireddy et al. (2022). Four optimizers were  
765 compared: FedAvg, FedAvgM, D-Byz-SGDM, and the heuristic momentum extension of Byz-  
766 VR-MARINA-PP (with  $\lambda \in \{10.0, 1.0, 0.1\}$ ) introduced in (Malinovsky et al., 2024), all using  
767 momentum parameter  $\alpha = 0.9$  where applicable. Training ran for 10 epochs (300 iterations total)  
768 for MNIST and 200 epochs for CIFAR-10, with results averaged over seeds  $\{0, 1, 2\}$ . For each  
769 optimizer we tuned the learning rate  $\eta \in \{0.1, 0.01, 0.001\}$ ; additionally Byz-VR-MARINA-PP  
770 tuned the clipping radius  $\lambda \in \{10.0, 1.0, 0.1\}$ . We selected the configuration with the highest mean  
771 validation accuracy across the three seeds for both the non-Byzantine and Byzantine experiments.  
772 Tables 1–4 provided complete configuration details.

773 **C.2 BASELINE PERFORMANCE EVALUATION**  
774

775 This experiment established baseline performance under partial participation without Byzantine  
776 clients across both MNIST (ConvNet) and CIFAR-10 (ResNet-18). We used  $n = 20$  clients with no  
777 Byzantine clients ( $\delta = 0$ ) and naive averaging aggregation. The objective was to validate that D-  
778 Byz-SGDM maintains competitive performance in non-Byzantine settings and to establish reference  
779 performance levels for subsequent robustness comparisons. Results in Figs. 2a and 2b demonstrated  
780 that D-Byz-SGDM outperformed standard momentum methods on both MNIST and CIFAR-10  
781 even without adversaries, suggesting that delayed momentum aggregation provided implicit regu-  
782 larization benefits under heterogeneous data distributions.

783 **C.3 BYZANTINE ROBUSTNESS ASSESSMENT**  
784

785 This experiment evaluated robustness against Byzantine attacks under partial participation on both  
786 datasets (MNIST with the ConvNet backbone and CIFAR-10 with ResNet-18). We configured  
787  $n = 25$  clients with 5 Byzantine clients (20%). Five robust aggregators were evaluated: Krum,  
788 coordinate-wise median, CCLIP (centered clipping), RFA, and naive averaging as baseline. The  
789 experimental design included both IID and non-IID data partitions, with bucketing applied in  
790 the Byzantine non-IID setting to mitigate extreme heterogeneity. This comprehensive evaluation  
791 spanned 6,480 total experimental runs across all combinations of attacks, aggregators, optimizers,  
792 data partitions, and random seeds (3,240 runs per dataset).

793 **C.4 NON-IID DATA PARTITION**  
794

795 We constructed the non-IID split following Karimireddy et al. (2022) in the *balanced* case: (i)  
796 sorted the training sets by label; (ii) split it into  $G$  equal, contiguous shards (where  $G$  is the number  
797 of good/honest clients); (iii) assigned one shard to each honest client and shuffle examples within  
798 each client. We partitioned the test set analogously.

800 **C.5 COMPUTING ENVIRONMENT**  
801

802 Experiments ran on NVIDIA A100-SXM4-80GB GPUs (CUDA 12.2) and AMD EPYC 7763 CPUs.  
803 Table 5 provides detailed hardware and software specifications.

804 **D EXTENDED RESULTS**  
805

806 **Per-aggregator curves with Byzantine clients.** This section complemented Figs. 1a and 1b by  
807 showing training dynamics for the other robust aggregators across the same attacks, data partitions,  
808 and optimizers on MNIST (ConvNet) and CIFAR-10 (ResNet-18).

810  
811  
812 Table 1: MNIST (non-Byzantine) configuration used in Fig. 2a.  
813  
814  
815  
816  
817  
818  
819  
820  
821  
822

Dataset	MNIST (IID and non-IID partitions)
Model	CONV-CONV-DROPOUT-FC-DROPOUT-FC
Clients	$n = 20$ (all honest)
Participation	$p = 0.5$ (partial participation)
Aggregator	avg
Batch size	32 per client
Training horizon	10 epochs (300 rounds)
Optimizers	FedAvg, FedAvgM, D-Byz-SGDM, Byz-VR-MARINA-PP
Learning-rate tuning	grid search on $\{0.1, 0.01, 0.001\}$
Byz-VR-MARINA-PP tuning	joint grid search $\eta \in \{0.1, 0.01, 0.001\}$ , $\lambda \in \{10.0, 1.0, 0.1\}$
Seeds	$\{0, 1, 2\}$
Attacks	none

823  
824 Table 2: MNIST (Byzantine) configuration used in Fig. 1a.  
825  
826  
827  
828  
829  
830  
831  
832  
833  
834  
835

Dataset	MNIST (IID and non-IID with bucketing $s = 2$ )
Model	CONV-CONV-DROPOUT-FC-DROPOUT-FC
Clients	$n = 25$ (20 honest, 5 Byzantine; $\delta = 0.2$ )
Participation	$p = 0.5$ (partial participation)
Aggregators	avg, krum, cm, CCLIP, rfa
Batch size	32 per client
Training horizon	10 epochs (300 rounds)
Attacks	BF, LF, mimic, IPM, ALIE, INF
Optimizers	FedAvg, FedAvgM, D-Byz-SGDM, Byz-VR-MARINA-PP
Learning-rate tuning	grid search on $\{0.1, 0.01, 0.001\}$
Byz-VR-MARINA-PP tuning	joint grid search $\eta \in \{0.1, 0.01, 0.001\}$ , $\lambda \in \{10.0, 1.0, 0.1\}$
Seeds	$\{0, 1, 2\}$

836 Notation: avg=naive average, krum=Krum (Blanchard et al., 2017a), cm=coordinate-wise median,  
837 CCLIP=centered clipping (Karimireddy et al., 2021), rfa=geometric median (RFA) (Pillutla et al., 2022).  
838  
839  
840  
841  
842  
843  
844  
845  
846  
847  
848  
849  
850  
851  
852  
853  
854  
855  
856  
857  
858  
859  
860  
861  
862  
863

864  
865  
866 Table 3: CIFAR-10 (non-Byzantine) configuration used in Fig. 2b.  
867  
868  
869  
870  
871  
872  
873  
874  
875  
876

Dataset	CIFAR-10 (IID and non-IID partitions)
Model	ResNet-18
Clients	$n = 20$ (all honest)
Participation	$p = 0.5$ (partial participation)
Aggregator	avg
Batch size	32 per client
Training horizon	200 epochs
Optimizers	FedAvg, FedAvgM, D-Byz-SGDM, Byz-VR-MARINA-PP
Learning-rate tuning	grid search on $\{0.1, 0.01, 0.001\}$
Byz-VR-MARINA-PP tuning	joint grid search $\eta \in \{0.1, 0.01, 0.001\}$ , $\lambda \in \{10.0, 1.0, 0.1\}$
Seeds	$\{0, 1, 2\}$
Attacks	none

877  
878 Table 4: CIFAR-10 (Byzantine) configuration used in Fig. 1b.  
879

Dataset	CIFAR-10 (IID and non-IID with bucketing $s = 2$ )
Model	ResNet-18
Clients	$n = 25$ (20 honest, 5 Byzantine; $\delta = 0.2$ )
Participation	$p = 0.5$ (partial participation)
Aggregators	avg, krum, cm, CCLIP, rfa
Batch size	32 per client
Training horizon	200 epochs
Attacks	BF, LF, mimic, IPM, ALIE, INF
Optimizers	FedAvg, FedAvgM, D-Byz-SGDM, Byz-VR-MARINA-PP
Learning-rate tuning	grid search on $\{0.1, 0.01, 0.001\}$
Byz-VR-MARINA-PP tuning	joint grid search $\eta \in \{0.1, 0.01, 0.001\}$ , $\lambda \in \{10.0, 1.0, 0.1\}$
Seeds	$\{0, 1, 2\}$

890 *Notation:* avg=naive average, krum=Krum (Blanchard et al., 2017a), cm=coordinate-wise median,  
891 CCLIP=centered clipping (Karimireddy et al., 2021), rfa=geometric median (RFA) (Pillutla et al., 2022).  
892  
893  
894  
895  
896  
897  
898  
899  
900  
901  
902  
903  
904  
905  
906  
907  
908  
909  
910  
911  
912  
913  
914  
915  
916  
917

Table 5: Runtime hardware and software.

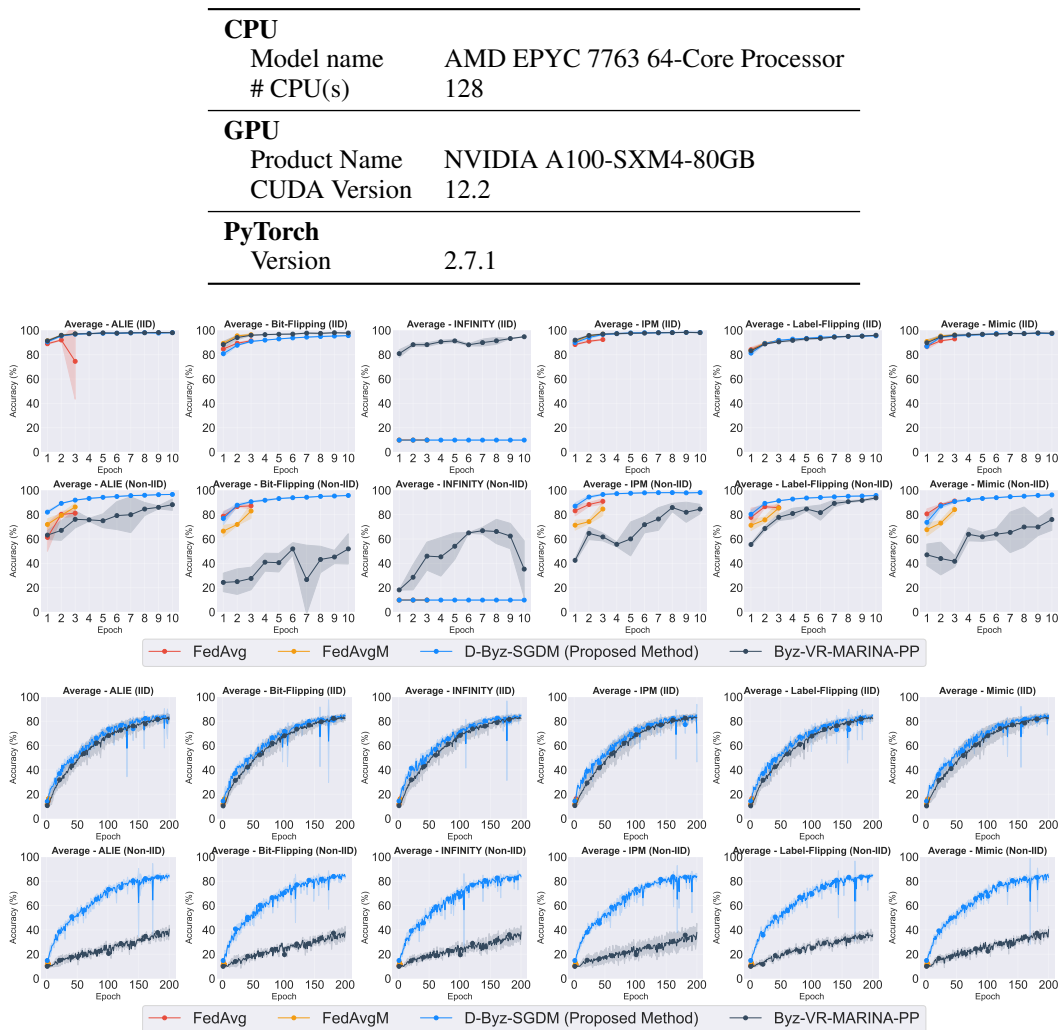


Figure 3: avg (naive average) under Byzantine attacks ( $p = 0.5$ ). The top row presents MNIST and the bottom row presents CIFAR-10; within each row the first strip is IID and the second strip is non-IID with bucketing  $s = 2$ . Columns proceed left to right through ALIE, Bit-Flipping, INFINITY, IPM, Label-Flipping, and Mimic.

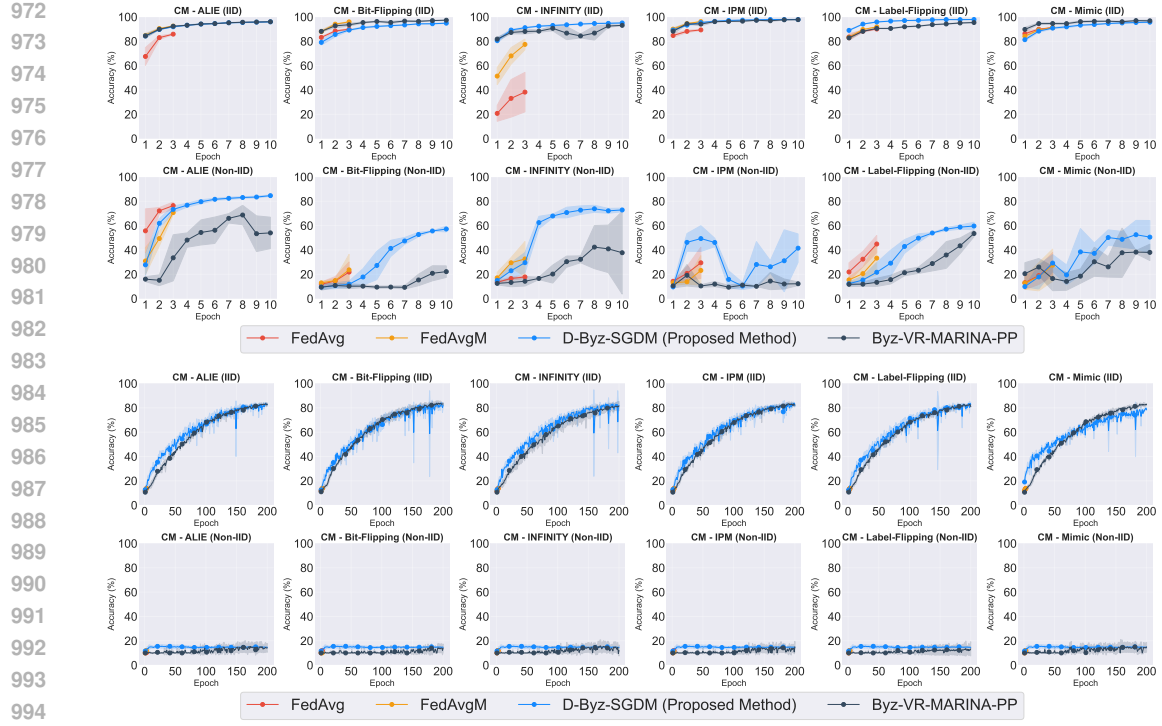


Figure 4: cm (coordinate-wise median) under Byzantine attacks ( $p = 0.5$ ). The layout matches Fig. 3: top row MNIST, bottom row CIFAR-10; within each row an IID strip is followed by a non-IID strip ( $s = 2$ ); columns move left to right through ALIE, Bit-Flipping, INFINITY, IPM, Label-Flipping, and Mimic.

995  
996  
997  
998  
999  
1000  
1001  
1002  
1003  
1004  
1005  
1006  
1007  
1008  
1009  
1010  
1011  
1012  
1013  
1014  
1015  
1016  
1017  
1018  
1019  
1020  
1021  
1022  
1023  
1024  
1025

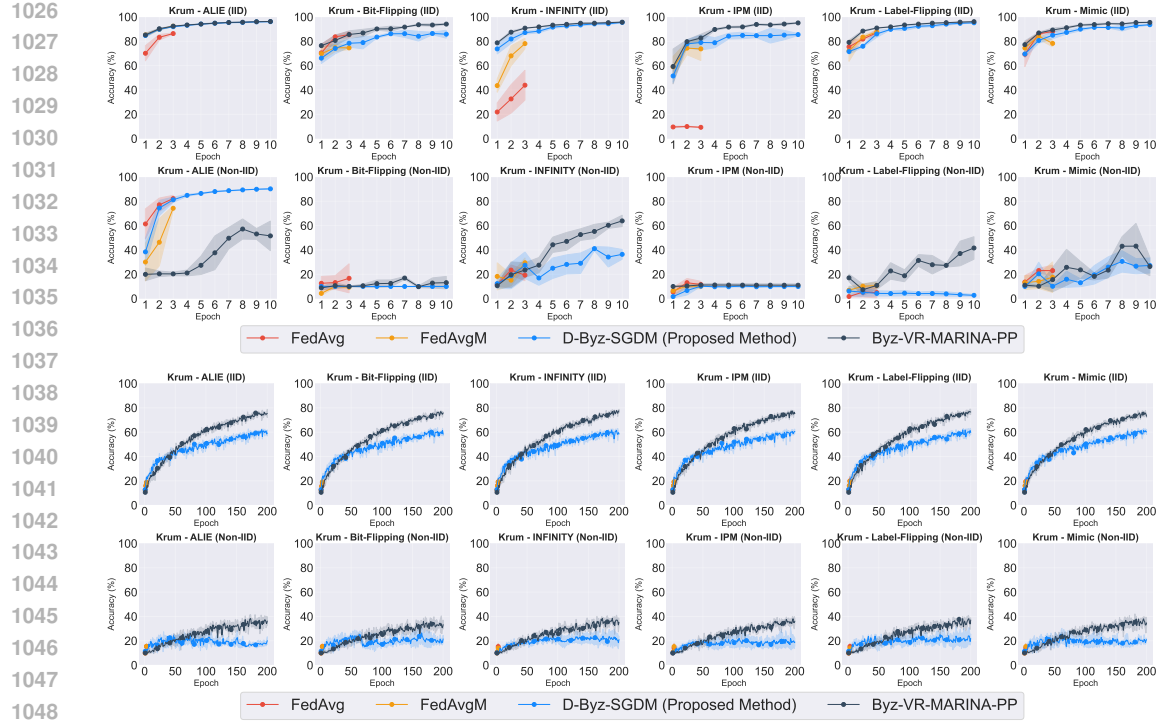


Figure 5: krum / Multi-Krum under Byzantine attacks ( $p = 0.5$ ). The top row shows MNIST and the bottom row shows CIFAR-10; each row contains an IID strip followed by a non-IID strip with bucketing  $s = 2$ . Columns list ALIE, Bit-Flipping, INFINITY, IPM, Label-Flipping, and Mimic.

1049  
1050  
1051  
1052  
1053  
1054  
1055  
1056  
1057  
1058  
1059  
1060  
1061  
1062  
1063  
1064  
1065  
1066  
1067  
1068  
1069  
1070  
1071  
1072  
1073  
1074  
1075  
1076  
1077  
1078  
1079

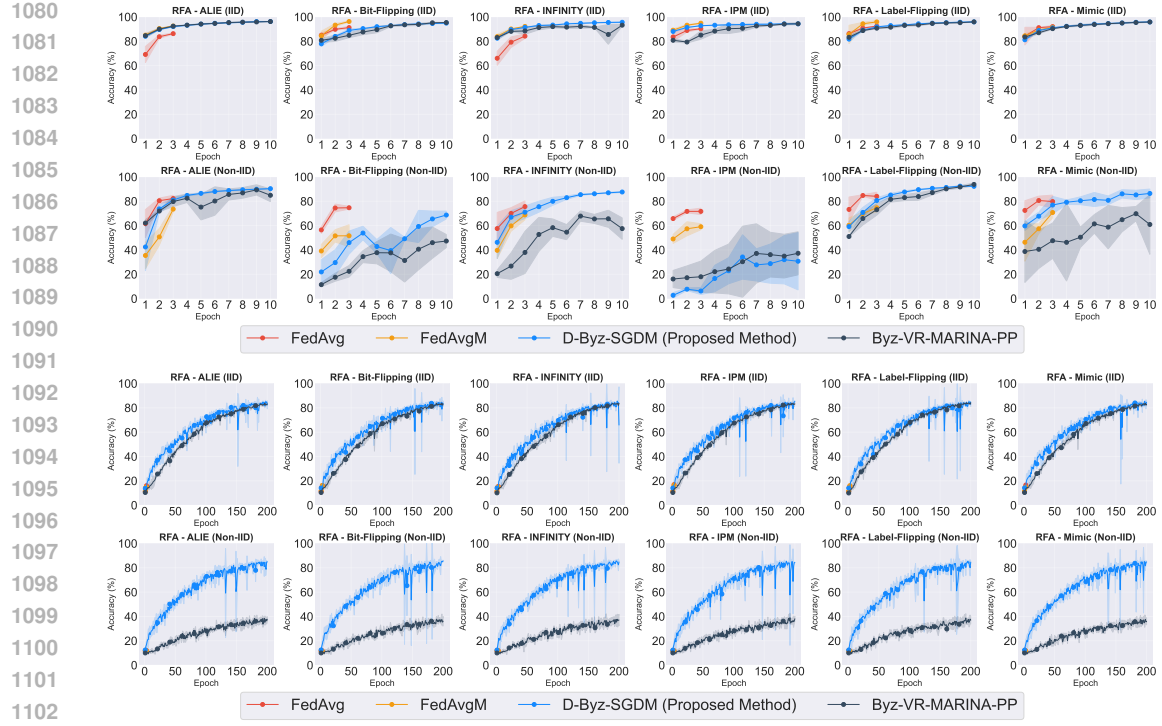


Figure 6: rfa (Robust Federated Averaging) under Byzantine attacks ( $p = 0.5$ ). The top row covers MNIST and the bottom row covers CIFAR-10; within each row an IID strip precedes a non-IID strip with bucketing  $s = 2$ . Columns run left to right through ALIE, Bit-Flipping, INFINITY, IPM, Label-Flipping, and Mimic.